Iron(III) Matrix Effects on Mineralization and Immobilization of Actinides

Cynthia-May S. Gong, Tyler A. Sullens, and Kenneth R. Czerwinski.

Harry Reid Center for Environmental Studies, University of Nevada, Las Vegas
4505 S. Maryland Parkway, Las Vegas, NV 89154-4009, USA

A number of models for the Yucca Mountain Project nuclear waste repository use studies of actinide sorption onto well-defined iron hydroxide materials. In the case of a waste containment leak, however, a complex interaction between dissolved waste forms and failed containment vessel components can lead to immediate precipitation of migratory iron and uranyl in the silicate rich near-field environment. Use of the Fe(III) and UO_2^{2+} complexing agent acetohydroxamic acid (AHA) as a colorimetric agent for visible spectrophotometry is well-known. Using the second derivative of these spectra a distinct shift in iron complexation in the presence of silicate is seen that is not seen with uranyl or alone. Silica also decreases the ability of uranyl and ferric solutions to absorb hydroxide, hastening precipitation. These ferric silicate precipitates are highly amorphous and soluble. Precipitates formed in the presence of uranyl below ~1 mol% exhibit lower solubility than precipitates from up to 50 mol % and of uranyl silicates alone.

INTRODUCTION

Yucca Mountain, located in Southern Nevada about 125 miles northwest of Las Vegas, has been under investigation as a potential national radioactive waste disposal site since the mid-1970s. It was chosen partly for its potential to act as a geologic barrier to waste migration due to a high water table and the maintenance of its near-field environment. Although it has been extensively characterized, the effects of actual storage cannot yet be known. Current regulations call for stringent engineering controls to prevent accidental radioactive and hazardous contamination to the surrounding geosphere for at least several centuries. The design of the future repository depends on the prediction of the waste-form behavior, and the accuracy of the prediction modeling scenarios depends in turn on the input parameters.

The repository characteristics are typically divided between "near field" and "far field" concerns. Our work concentrates on the chemistry at the near field, the environment immediately surrounding the waste packages, with particular emphasis on the impact of iron leachate and the environmental matrix on the behavior and speciation of the actinide components. Actinides are the species of main concern for the radioactive profile of the Yucca Mountain site. Environmental contamination by actinides could result from a barrier or containment failure, which may be expected to contain a high concentration of iron. While ferric iron (Fe(III)) tends to precipitate quickly, ferrous iron (Fe(II)) is much more soluble, leading to a complex interplay of both oxidation states. Uranium, however, is typically in the form of uranyl, $U(VI)O_2^{2+}$, the only oxidation state soluble enough to be considered mobile. The tuff surrounding Yucca Mountain contains a large amount of calcium - from 0.3 mM in J-13 well water up to 2.2 mM in UE-25p well water -, and measurable concentrations of the other alkali earths. Finally, silicon and carbonate are present at high concentrations in the groundwater and environmental matrix; silicon is present in millimolar concentrations, and carbonate is documented at 15 mM and higher.

The migration of actinides through the environment may be retarded by mineral formation and sorption onto mineral surfaces, especially iron minerals. A number of toxic metals, including uranium, are known to coprecipitate with ferric iron. Previous alteration phase work mostly focuses on Fe(III) without cataloguing the effects of the silica and calcium. Under highly alkaline conditions at elevated temperatures (up to 70 C), these iron oxyhydroxides can over time incorporate uranate and then form heterogeneous mineral phases with schoepite. A migration of solubilized uranyl waste and ferric leachate is likelier to

immediately contact ambient temperature groundwaters with varying pH and a dissolved mineral matrix. The thermodynamics are vastly different under these conditions, and kinetics dominates the mineral formation.

As part of a larger project that includes the effects of the iron oxidation state and dissolution of the alteration phases, the work presented explores the mineralization of uranium at varying pH in the presence of ferric iron and silicon. The solid precipitates are characterized using a variety of methods including x-ray diffraction (XRD), UV-visible spectroscopy (UV-vis), and other spectroscopy.

WORK DESCRIPTION

All solutions were prepared within a week of use. Iron(III) chloride, sodium metasilicate, and calcium chloride were obtained from Alfa Aesar. Fifty millimolar stock solutions were prepared from solids.. Uranyl nitrate was diluted from a 1.0 M stock. Alpha hydroxamic acid (AHA) was procured from Aldrich and prepared fresh before each run. All solutions were dissolved in deionized water and the U, Fe, and Si stocks were pushed through 0.45 um polypropylene filters prior to use. Nitric acid stocks were prepared from JT Baker reagent grade. A concentrated sodium hydroxide stock was prepared from dried solids and tested against standardized nitric acid. Diluted titration solutions were prepared from these stocks. ICP-AES standards were obtained from NIST and prepared as directed.

Titrations were performed using calibrated pipettes and a Brinkmann Metrohm Titrino 799. The titrated concentrations of Iron(III), and uranyl were varied systematically up to 2 mM, both with 1mM silica and in its absence. The molar ratio of uranium to iron was varied from 0.5% to 50%.

Precipitates were generated by addition of NaOH or by contact with matrix water simulant at pH values of 4 to 9. Wet aged samples were maintained in a minimum of supernatant at ambient temperature for over two months. Solution concentrations were determined using a Spectro Ciros ICP-AES. A PANalytical X'Pert PRO X-ray diffractometer with an X'Celerator detector was used for the XRD experiments.

A Cary 6000 spectrophotometer was used for the UV-vis measurements and derivative calculations. The UV-vis spectra were taken in the presence and absence of 0.05 mM AHA; the three components were varied systematically from 0.05 to 5 mM. The behavior was compared to that of the independent elements as well as combinations of two elements. The solutions were made up to concentration and the AHA solution was added to each cuvette approximately 10 seconds before the spectrum was taken to ensure that the non-decomposed component was constant across samples.

RESULTS

The formation of minerals as secondary alteration phases is highly dependent on pH, total concentration, molar ratios, and aging. Contact of ferric and uranyl solutions with silicate-rich matrix water and titration of the ferric silicate systems indicate a large effect of silicate on mineralization and precipitate solubility.

As is expected from the solubility constant of ferric hydroxide (~$4x10^{-38}$at 25 C), the iron-containing precipitates were iron-driven and began to precipitate around pH 2.4-2.5. The presence of silica delays the onset of precipitation by about 0.1 pH unit (1:1 molar ratio). The presence of uranyl, once it has reached a minimum 25 mol% to iron, delays the onset of precipitation even further – up to 1 pH unit at 50 mol%, where the ferric hydroxide begins to precipitate at a pH of ~3.4.

[U] (mM)	[Fe] (mM)	[Si] (mM)	1st i.p.	2nd i.p.	Onset of ppt
0	2	1	2.45		2.43
0.01	2	1	2.45		2.53
0.02	2	1	2.50		2.48
0.04	2	1	2.46	4.8	2.46
0.10	2	1	2.60	4.6	2.52
0.40	2	1	2.57	4.6	2.62
1.0	2	1	2.52	4.6	3.20
0.1	0	1	3.5 (sl.)		n/a
1	0	1	3.1	4.5	n/a
1	0	0	4.3	6.5	n/a
10	0	0	4.3	5.6	5.35

Table 1: Inflection points of titrated solutions. The presence of uranyl at a concentration above a set point enhanced the ability of the ferric silicates to absorb hydroxide ions without precipitation, shifting the titration curve.

Interestingly, as the concentration of uranyl began to exceed 0.04 mM (2 mol%), an additional point of inflection appeared on the titration curve (Table 1). Concentrations shown reflect beginning concentrations. All solutions were titrated from an initial pH of 2.05 ± 0.05.

The presence of silica affects the ability of iron(III) and uranyl to incorporate hydroxyl ions into their precipitates, as evidenced by a significantly reduced titrant requirement. The presence of uranyl has a significant effect on ferric hydroxide precipitation as well, shifting the titration curve to the left (Figure 1).

Although the presence of silica seems to have no effect on the precipitation of uranyl without iron, it has a distinct effect on the inflection points. Uranyl without silica can absorb about 50% more base at without the pH rising above 2-3 than the same concentration with silica. The silica interacts immediately with both the uranyl and iron complexes. Addition of silica to dissolved iron, normally a pale yellow solution at these concentrations, shifts the color to a deep orange.

The complexing agent AHA is often used as a reductant for higher oxidation states of plutonium and neptunium. It also complexes, but does not reduce, uranyl ions. AHA is unstable, however, especially in acidic media; it decomposes quickly to acetic acid and hydroxylamine. AHA is also known to strongly complex to Fe(III), Al(III), and some lanthanides. The complexation of uranyl by AHA does not significantly alter the UV-vis spectrum of the aqueous compound, though it enhances the signal. The addition of silicate has little additional effect, though some peaks are skewed and the background is higher. AHA does not complex silica on its own.

A real difference can be seen in a 1 mM Fe(III)-AHA complex by varying the silica. Addition of the AHA, again, does not shift the visible spectrum, but adding silica does. The shift is noticeable in the raw absorbance data, but transformation into the second derivative clarifies the shift in iron complexation: as the ratio of silica to iron increases from zero to 5, a peak at 435 nm begins to grow (Figure 2); it is noticeable when the Fe:Si ratio is as low as 4:1, but all of the iron shifts to the silicate complex when the concentration of

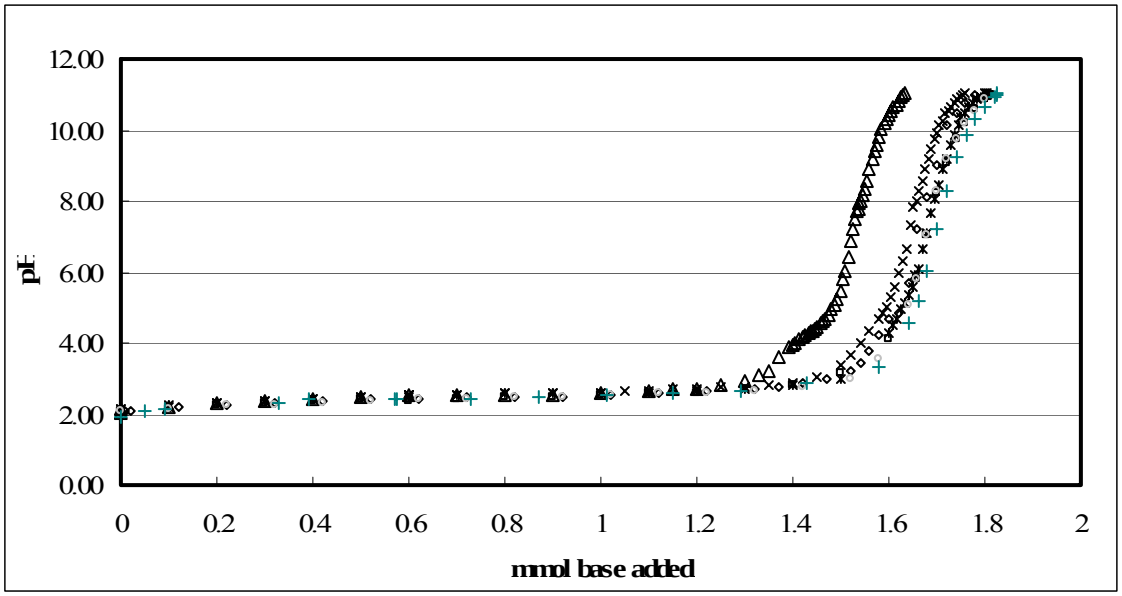

Figure 1: Dependence onUO_2^{2+} of an Iron(III)-Silicate system. All titrated solutions have 1 mM Si and 2 mM Fe and were begun at pH 2.05 ± 0.05. Uranyl concentrations varied as follows: Δ 1 mM; x 0.4 mM; * 0.1 mM; ♦0.04 mM; □ 0.02 mM; ◊ 0.01 mM; and + no uranyl. We see that there is little effect until the molar ratio of uranyl to iron exceeds 5%, the point at which in the literature ferric hydroxide ceases to sorb uranyl.

silica is as high as iron.

Mixing the three components is interesting. The relative stability constants of the ferric- and uranyl-AHA complexes suggest that the ligand strongly prefers the ferric ion to uranyl; using the first derivative of the spectrum, we can detect characteristics of uranyl in a mixture with silica even when iron is in five times molar excess (Figure 3). The stability constant of Fe(III)-AHA is four orders of magnitude greater than that of uranyl-AHA, and the extinction coefficient of the free Fe(III) ion is at least two orders of magnitude greater than uranyl nitrate. The observed phenomenon may be due to a different dynamic in AHA binding to ferric and uranyl silicates.

The precipitates were qualitatively analyzed using X-ray powder diffraction techniques. The samples were amorphous and remained so even after aging for over two months in a wet slurry, so a diagnostic XRD pattern could not be obtained. These amorphous solids redissolved easily, even in NaOH solutions as high as 0.1 M. Over time, the supernatant tended to become more acidic, presumably as the structures rearranged and took up more ambient hydroxides. For the low pH experiments with high uranyl concentration, the initial precipitates could redissolve as the pH dropped below ~3.5 from 4.0. The rearrangement of the structure still did not achieve enough crystallinity for a significant XRD interpretation.

CONCLUSIONS

Although ferric-uranyl hydroxide studies have been extensively studied, in the context of Yucca Mountain near-field modeling, the effects of silica and other matrix components have a significant impact on the mineralization, precipitation, and solubility that has not been sufficiently recognized. The presence of silica with either iron or uranyl decreases the ability of each to absorb hydroxyl ions, and UV-vis data show a clear shift in the iron spectrum, indicating a strong complexation. The incorporation and sorption of uranyl into ferric hydroxides is well studied, but a better model may be its interaction with iron silicates

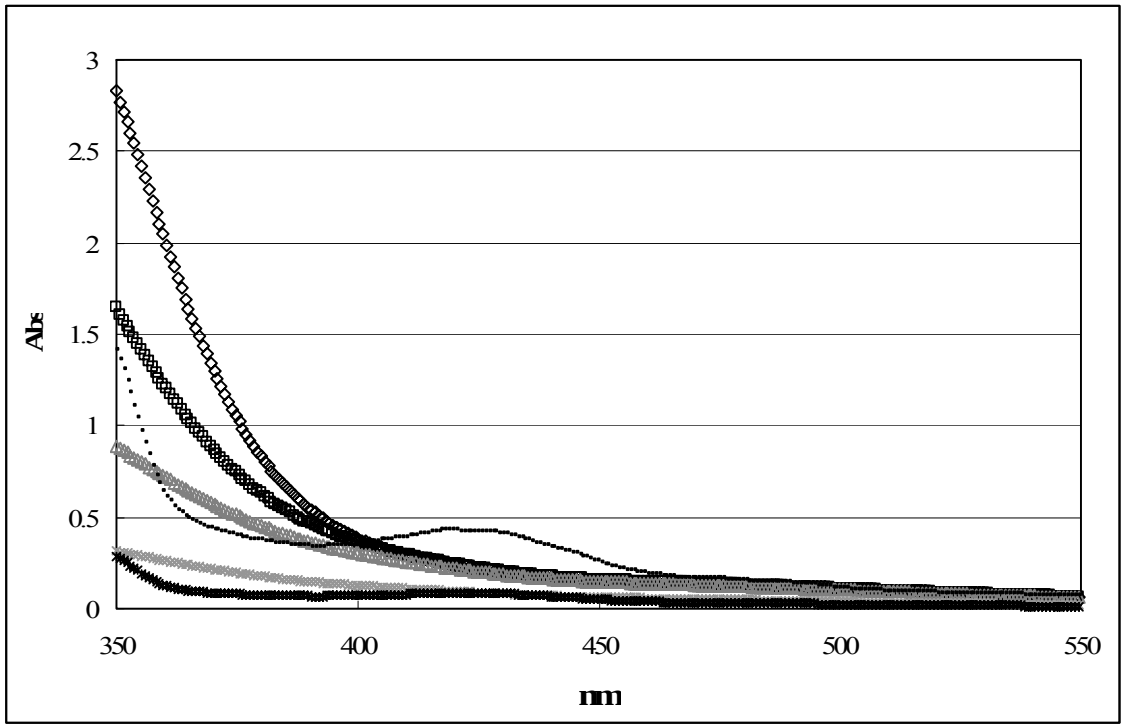

Figure 2: Effects of Fe(III) on the U(VI)-Si-AHA visible spectrum. As the concentration of iron decreases, the uranyl character of the visible spectrum emerges. UO_2^{2+} and Si are held at 1 mM: ◊ 5 mM Fe; □ 2.5 mM Fe; Δ 1 mM Fe; x 0.25 mM Fe; * 0.05 mM Fe; ▪ 0.05 mM Fe (5x amplified).

The mineral precipitation in the iron (III) system is clearly driven by the insolubility of ferric hydroxide. This is in contrast to the iron (II) system, also being studied in our laboratory, in which precipitation is driven by uranyl and mineralization does not begin until a much higher pH. The presence of uranyl delays the onset of precipitation and also shifts the titration curve to the left. This is the opposite of the expected effect of independent precipitation, where the two elements would compete for hydroxide. This indicates an incorporation of uranyl into the structure of the ferric hydroxides.

The amorphous nature of the precipitations is dominant at both iron oxidation states, however. The solubility of amorphous minerals can be orders of magnitude greater than of crystalline, which has implications for the control of actinide migration. Wet aging at ambient temperature maintained at pH up to 9 for over two months did not enhance crystallinity; studies are underway to determine whether the thermodynamic product produced by dry aging at different temperatures will form hematite or goethite, as in the literature. The presence of silica is likely to be a factor in the ordering of the crystals.

The titration inflection point around pH 2.4 is due to the precipitation of $Fe(OH)_3$ and $Fe(SiO_4)OH$. The second inflection, around 4.6, is due to the precipitation of excess $UO_2(OH)_2*xH_2O$. Interestingly, although the inflection point did not change for the iron in the presence of uranyl and/or silicate, the amount of base necessary to raise the pH of the systems *decreased* with increasing uranyl concentration. This is counterintuitive, as one would assume that the uranyl would act as a competitor with the iron for hydroxide. This may suggests a displacement of hydroxide in the iron mineral formation. The slow reacidification of the samples during wet aging may reflect the thermodynamic rearrangement to ferric hydroxides. Previous work (1) has shown that under certain circumstances ferric hydroxides can incorporate up to 0.6 mol % uranate, followed by surface sorption.

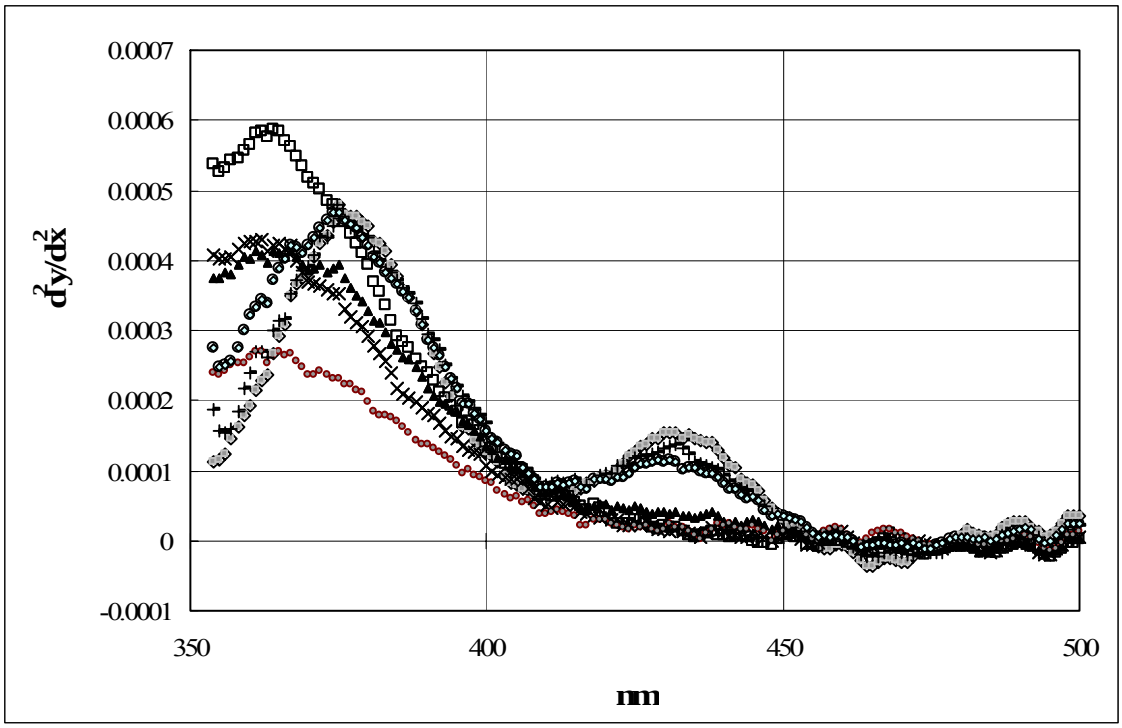

Figure 3: Effect of silicate on Fe(III)-AHA second derivative spectra. At a constant 1 mM ferric concentration, with and without AHA, the concentration of silica affects the second derivative of the visible spectrum. As Si increases past a molar ratio of 4:1 Fe:Si, the peak redshifts and second peak at 435 nm appears. Without AHA: ● no Si; ◊ 1 mM Si. With 0.05 mM AHA: □ no Si; x 0.05 mM Si; ▲0.25 mM Si; + 1 mM Si; ♦ 5 mM Si.

Our studies with the ferric silicates indicate a similar mechanism, with further excess uranyl complexing silicate and precipitating in turn.

The use of the second derivative of AHA complex visible spectra to simultaneously characterize Fe^{3+} and UO_2^{2+} complexation is an intriguing new tool that should be explored. The clear shift in the second derivative Fe(III)-AHA peak upon ferric complexation is of especial interest. We are pursuing a more thorough study to determine the threshold concentration of silicate for this peak to form and the optimal conditions to discriminate between the free iron and the complexed iron silicate. It remains to be seen whether this method can be used to quantify or even qualify uranyl complexation in the presence of iron. Other ligands are also being explored for their potential as colorimetric tools to differentiate iron and uranyl complexes.

ACKNOWLEDGMENTS

The authors acknowledge the Department of Energy Cooperative Agreement DE-FC28-04RW12237 for funding. The authors would also like to acknowledge Jeanette Daniels for her invaluable assistance.

REFERENCES

(1) Duff, M. C., Coughlin, J. U., and Hunter, D. B. (2002) Uranium co-precipitation with iron oxide minerals. *Geochim. Cosmochim. Acta* 66(20), 3533-3547.